Journal of Volcanology and Geothermal Research 251 (2013) 149–157

Contents lists available at SciVerse ScienceDirect

Journal of Volcanology and Geothermal Research

journal homepage: www.elsevier.com/locate/jvolgeores

Forecasting seismic scenarios on Etna volcano (Italy) through probabilistic intensity attenuation models: A Bayesian approach

R. Azzaro [a,*], S. D'Amico [a], R. Rotondi [b], T. Tuvè [a], G. Zonno [c]

[a] Istituto Nazionale di Geofisica e Vulcanologia, Osservatorio Etneo, Piazza Roma 2, 95123, Catania, Italy
[b] C.N.R.—Istituto di Matematica Applicata e Tecnologie Informatiche, via Bassini 15, 20133, Milano, Italy
[c] Istituto Nazionale di Geofisica e Vulcanologia, Sezione di Milano–Pavia, via Bassini 15, 20133, Milano, Italy

ARTICLE INFO

Article history:
Received 20 May 2011
Accepted 25 July 2012
Available online 1 August 2012

Keywords:
Macroseismic intensity
Attenuation
Probability distribution
Source models
Seismic scenario
Mt. Etna

ABSTRACT

In this paper, we apply a probabilistic procedure to model the attenuation of the macroseismic intensity in the Mt. Etna region, which allows estimating probabilistic seismic scenarios. Starting from the local earthquake catalogue, we select a dataset of 47 events having epicentral intensity I_0 from VI to IX–X EMS, and update the model parameters previously achieved for Italy according to the Bayesian paradigm. For each class of epicentral intensity I_0, we then estimate the probability distribution of the intensity at a site conditioned on the epicentre-site distance through a binomial-beta model, under the assumption of a point seismic source and isotropic decay (circular). The mode of the distribution is taken as the expected intensity I_s at that site. Since the strongest earthquakes show a preferential propagation of shaking along the fault strike and a rapid decrease in the perpendicular direction, we also consider the anisotropic decay (elliptical) of the intensity due to a linear source (finite fault). We therefore transform the plane so that the ellipse has the length of the fault rupture as maximum axis and its strike as azimuth is changed into a circle with fixed diameter; then we apply the probabilistic model obtained for the isotropic case to the modified data. The entire calculation procedure is implemented in the software PROSCEN which, given the location and the epicentral intensity (and eventually the fault parameters) of the earthquake to be simulated, generates the probabilistic seismic scenario according to the isotropic and anisotropic models of attenuation. The results can be plotted on grid maps representing (1) the intensity that can be exceeded with a fixed probability, or (2) the probability of exceeding a fixed intensity value. The first representation may also find application in seismic monitoring at Etna volcano, in order to produce real-time intensity ShakeMaps based on the instrumental parameters calculated by the automatic earthquake processing system.

1. Introduction

Simulating the effects produced by an earthquake is a multidisciplinary field of investigation aimed at assessing the level of seismic risk to which an area is exposed and preparing emergency plans. A variety of methods, leading to deterministic or probabilistic seismic scenarios, have been developed according to different levels of accuracy required — the most complete generally being based on numerical models that take account of ground-motion predictive relationships (expressed in acceleration, velocity or displacement), local geologic conditions (site effects), historical macroseismic intensity data, together with building typologies and their vulnerability. These seismic scenarios are normally envisaged for large cities and refer to the strongest earthquakes or their occurrence probability (for an overview in Europe, see Faccioli, 2006 and references herein). Regarding volcanic regions, a few applications have focused on Mts. Etna (Faccioli et al., 1999) and Vesuvius (Galluzzo et al., 2008), Iceland (Sigbjörnsson et al., 2007) and the Azores Islands (Zonno et al., 2010) with varying degrees of detail.

On the other hand, a simplified approach adopted worldwide to provide a preliminary, semi-quantitative assessment of the level of shaking and extent of potential earthquake hazard is obtained through the software package ShakeMap (Wald et al., 1999). This procedure seeks to automatically estimate, in a few minutes, the level of expected ground shaking using real-time data acquired by a seismic network, which are converted into maps of peak ground acceleration (PGA), peak ground velocity (PGV) and macroseismic intensity. The last parameter, in particular, is the most used for non-specialist applications of civil protection to evaluate simplified scenarios in support of possible actions of first intervention. Its application in Italy is quite recent (Michelini et al., 2008), namely the Centro Nazionale Terremoti—INGV producing real-time MCS intensity maps for $M_L > 3.0$ earthquakes (http://earthquake.rm.ingv.it/shakemap/shake/index.html). The 'instrumental intensity' values deriving from the conversion of PGA–PGV parameters, are obtained through correlation relationships calibrated for the national territory (Faenza and Michelini, 2010).

* Corresponding author. Tel.: +39 957165821.
E-mail address: azzaro@ct.ingv.it (R. Azzaro).

0377-0273/$ – see front matter © 2012 Elsevier B.V. All rights reserved.
http://dx.doi.org/10.1016/j.jvolgeores.2012.07.011

However, ShakeMap cannot be used at Etna due to the different attenuation and scaling laws of tectonic events vs volcanic earthquakes (Rovelli et al., 1988; McNutt, 2005; Giampiccolo et al., 2007). Milana et al. (2008) therefore proposed an alternative procedure aimed at identifying, in near-real time, potentially damaging earthquakes starting from the value of the instrumentally determined magnitude. Through the computation of pseudo-velocity response spectra, this method provides a preliminary estimate of the macroseismic intensity at the epicentre (I_0), but it does not reproduce the areal distribution of the expected intensities. However, it must be stressed that these two methods are based on a succession of conversion relationships from instrumental ground-motion parameters into macroseismic intensity.

In this paper, we tackle the problem of seismic scenarios at Etna entirely in terms of macroseismic intensity, exploiting as best as we can on the huge amount of data available from the local historical earthquake catalogue (Azzaro et al., 2000). By adopting a probabilistic approach based on the Bayesian statistics (Rotondi and Zonno, 2004), we analyse the decay of the intensity from the source according to the two attenuation models, isotropic (point source, symmetric decay) and anisotropic (linear source, decay depending on the direction), and calculate the probability distribution of the intensity at a given site (I_s) conditioned on the epicentral intensity (I_0) of the earthquake and the epicentre-site distance through a binomial-beta model (Zonno et al., 2009). The backward validation of the results and comparisons with simulations from a deterministic approach, are also presented. The entire procedure is finally implemented in software to produce probabilistic ShakeMaps expressed in terms of macroseismic intensity. This application is proposed as a practical tool to be applied at INGV—Catania data acquisition centre for obtaining real-time seismic scenarios at Etna.

2. Intensity attenuation: conceptual background and input data

The problem of the macroseismic intensity attenuation and its variation as a function of the distance from the source, is a key element in seismic hazard assessment (Albarello and D'Amico, 2004, 2005; Pasolini et al., 2008a). This issue has widely been analysed from the deterministic point of view by applying linear regressions which express the intensity at site (I_s) as a function of the epicentre-site distance, the epicentral intensity I_0 and other factors like the depth; to take into account the wide scatter of the observations around the expected values, these relationships may be provided with a gaussian error. Pasolini et al. (2008b and references herein) recently calculated a unique attenuation pattern for the whole of Italy according to an isotropic model of decay, which has the obvious limitation of not considering different regional attenuation trends, source directionality, or possible local effects. On the other hand, Azzaro et al. (2006) derived specific regression relationships for the intensity attenuation in the volcanic districts, finding for Etna an intensity decay ΔI (the difference between I_0 and I_s) of 4 degrees in 20 km of distance from the epicentre, under the same assumption of isotropic model (i.e. point source). In general, this determines highly localised macroseismic effects with respect to the tectonic earthquakes occurring in the national territory. Moreover, the same authors also pointed out the importance of the anisotropy due to a linear source in the attenuation pattern, which at Etna is characterised by a preferential propagation (i.e. highest intensities) along the fault strike and a rapid decrease of the effects in the perpendicular direction. The decay of intensity, given by the difference between maximum and minimum attenuation, reaches 2 intensity degrees at equal distances from the epicentre. As a result, the mesoseismal areas appear typically elliptical, with extensions up to 5 km long and 2 km wide astride the causative fault (Azzaro, 2004). Taking the strike of the source into account is therefore important for modelling hazard scenarios in the near-field, where the expected effects have to be simulated as realistically as possible.

The probabilistic approach to the analysis of the seismic attenuation has been developed in order to quantify the intrinsic uncertainty of the decay process (Magri et al., 1994; Albarello and D'Amico, 2005). In Zonno et al. (1995) the intensity decay ΔI, normalised on I_0, is considered as a random variable that follows a Beta distribution with the mean proportional to a known attenuation law and deviation depending on the distance from the epicentre. Then, avoiding the use of any deterministic attenuation relationship, Rotondi and Zonno (2004) proposed another probabilistic model calibrated by exploiting information from zones that, on the basis of their seismotectonic features, are assumed as homogeneous from the viewpoint of attenuation. This debatable assumption was replaced in Rotondi et al. (2008), Zonno et al. (2009) by a hierarchical agglomerative clustering method employed to separate a set of representative macroseismic fields – the so called learning dataset – into homogeneous groups from the viewpoint of attenuation. In this way, three classes with decreasing attenuation (C_A, C_B, C_C) have been identified in Italy, and in each of them the probability distributions of I_s conditioned on the epicentral intensity I_0 and the epicentre-site distance, were estimated. Because of the higher attenuation of seismic intensity (Azzaro et al., 2006), the Italian volcanic areas were excluded from these analyses.

The application of the probabilistic procedure of attenuation at Etna volcano requires an ad-hoc calibration of some parameters through a reference macroseismic dataset. To this end, we use the most updated release of the macroseismic catalogue of Mt. Etna earthquakes (CMTE Working Group, 2008). It represents a homogeneous macroseismic database compiled through the revision of the original coeval sources, intensity assigned by using the European macroseismic scale (EMS, Grünthal, 1998) and epicentral parameters defined according to standard procedures. Unlike the Italian seismic catalogue (CPTI Working Group, 2004), it does not adopt any intensity threshold (or equivalent magnitude) and reports, for the major events, the association seismogenic fault-earthquake defined on the basis of occurrence of coseismic surface faulting (Azzaro, 1999), or the distribution of the highest intensities with respect to the tectonic pattern (Azzaro, 2004). These last features, together with the aforementioned very high intensity decay with distance, ensure that the accuracy of the epicentre locations in densely urbanised areas is fairly high, with errors around 1 km.

In order to limit the uncertainties due to poorly constrained parameters, we select a set of 47 events with epicentral intensity $I_0 \geq$ VI EMS and macroseismic fields characterised by a uniform distribution of the intensity data points (N_{ip}); the related intensity database consists of 1403 macroseismic observations regarding 229 localities. As shown in Fig. 1, this selection includes most of the destructive or severely damaging earthquakes occurring at Etna, which struck localities very close to each other in the eastern flank of the volcano. These events are mainly due to the activity of the Timpe fault system (Azzaro, 2004).

In particular, for the isotropic model (point source) we use 44 earthquakes with $N_{ip} \geq 10$, while for the anisotropic model (linear source) we analyse a slightly different subset consisting of 17 events with $I_0 \geq$ VII EMS and $N_{ip} \geq 7$; the dataset is reported in Table 1 (for brevity, the events with $I_0 =$ VI EMS are only listed in the caption). For the purposes of our analysis, the values of I_0 expressed with an intensity range (VII–VIII, VIII–IX etc) are assumed as being of lower degree; such a choice is due to a non-representative distribution of the highest intensity data points in the macroseismic field.

3. Binomial-beta model for macroseismic intensity at a site

3.1. Isotropic model

In this paragraph, we deal with seismic attenuation under the assumption of point source model; this means that in the simulated

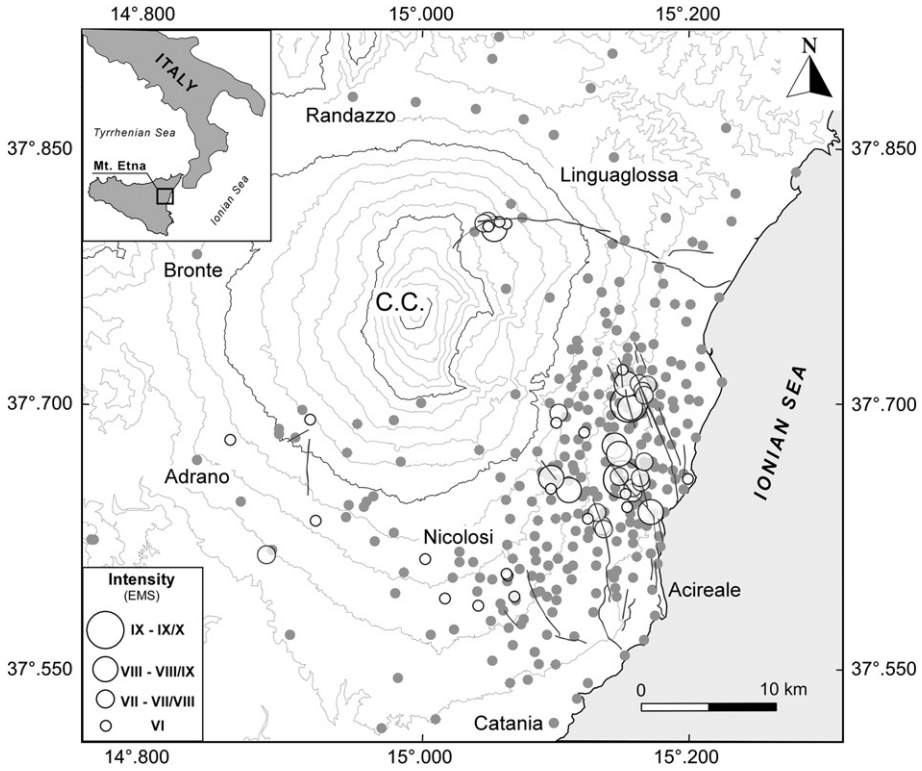

Fig. 1. Distribution of the epicentres (circles) of the 47 earthquakes with $I_0 \geq$ VI used in this study (see Table 1). The localities (grey dots) represented in the macroseismic fields and the seismogenic faults, are also reported.

macroseismic field the isoseismal lines bounding the points of equal intensity, are circular. Zonno et al. (2008) and Rotondi et al. (2009) carried out an analysis on representative macroseismic dataset of 38 earthquakes from different volcanic areas of Italy by computing, for each macroseismic field, median, mean and third quartile of the distances epicentre-site related to the same decay ΔI class ($\Delta I = 0,1,\ldots, I_0 - 1$). These values were collected in a $(n \times 3 \max I_0) = (38 \times 30)$ matrix, n being the number of the earthquakes, and then applied a hierarchical agglomerative clustering method (Kaufman and Rousseeuw, 1990) implemented in the free software R (R Development Core Team, 2008) by the AGNES (AGglomerative NESting hierarchical clustering) routine in order to group the macroseismic fields according to different attenuation trends. On the basis of the comparison with the class C_A of earthquakes determined in Zonno et al. (2009) to have the highest attenuation in the tectonic areas, it appeared that the similar decay trend may be used for the Etna region if the width of the distance bins is reduced by the factor 10, and for other volcanic districts by the factor 2. We will use this information to assign prior probabilities in the following.

In the probabilistic model proposed by Rotondi and Zonno (2004), as the variable ΔI is discrete and belongs to the domain $\{0, I_0 - 1\}$, it is reasonable to choose for $I_s = I_0 - \Delta I$, at a fixed distance from the epicentre, the binomial distribution $\mathrm{Bin}(i_s \mid I_0, p)$ depending on I_0 and the parameter $p \in (0,1)$:

$$Pr\{I_s = i | I_0 = i_0, p\} = \binom{i_0}{i} p^i (1-p)^{i_0 - i} \qquad i \in \{0, 1, \ldots, i_0\} \tag{1}$$

and then restrict the support to be $\{1, I_0\}$ by defining $Pr\{I_s = 1\} = Pr\{I_s \leq 1\}$. Moreover, since the ground shaking may differ even among sites located at the same distance, we consider p as a random variable which follows a Beta distribution:

$$Be(p; \alpha, \beta) = \frac{\Gamma(\alpha+\beta)}{\Gamma(\alpha)\Gamma(\beta)} \int_0^p x^{\alpha-1}(1-x)^{\beta-1} dx \tag{2}$$

where α and β are the parameters which, according to the Bayesian paradigm, must be assigned to express our prior knowledge. To this end, we draw L distance bins R_j, $j = 1,2,\ldots,L$, of fixed width around the epicentre of each earthquake and assume that, in all the sites within each jth distance bin, I_s has the same binomial distribution with parameter p_j, which, in turn, follows the distribution $\mathrm{Beta}(\alpha_{j0}, \beta_{j0})$. We assign to the prior parameters α_{j0}, β_{j0} the values obtained for α_j, β_j parameters of the posterior distribution of p_j in the class C_A and use, for L distance, a distance bin of 1 km wide. This value is comparable with the error of the epicentre location of the selected events, and with the distance found by Azzaro et al. (2006) to correspond to the decay $\Delta I = 1$.

Using the earthquake dataset in Table 1 (isotropic model), we then improve our knowledge on the attenuation process; formally, for a fixed I_0, through Bayes' theorem we update the parameter values in the distance bin R_j, $j = 1,2,\ldots,L$ by:

$$\alpha_j = \alpha_{j0} + \sum_{n=1}^{N_j} i_s^{(n)} \qquad \beta_j = \beta_{j0} + \sum_{n=1}^{N_j} \left(I_0 - i_s^{(n)}\right) \tag{3}$$

where N_j is the total number of data points D_j inside R_j and $i_s^{(n)}$ is the intensity felt at the n-th site. Moreover, we estimate p_j through its posterior mean:

$$\hat{p}_j = E\left(p_j \middle| D_j\right) = \frac{\alpha_{j,0} + \sum_{n=1}^{N_j} i_s^{(n)}}{a_{j,0} + \beta_{J,0} + I_0 \cdot N_j}. \tag{4}$$

In order to let the p parameter of the binomial distribution for the site intensity I_s varies with continuity, we smooth the estimates $\hat{p}_j, j = 1, \ldots, L$ with the method of least squares, using an inverse power function $g(d) = (\gamma_1/d)^{\gamma_2}$. In this way it is possible to assign the binomial probability of I_s at any d distance from the epicentre by:

$$Pr_{\mathrm{bin}}\{I_s = i | I_0; g(d)\} = \binom{I_0}{i} g(d)^i (1-g(d))^{I_0 - i} \qquad i \in \{0, 1, \ldots, I_0\} \tag{5}$$

Table 1
Dataset of the earthquakes used in this study, and related parameters (from CMTE Working Group, 2008). Blanks indicate earthquakes not used in that specific model. I_0, epicentral intensity; E_0, epicentre, expressed as the barycentre of the data points with intensity I_0, I_0-1, while in cases of earthquakes accompanied by coseismic faulting, it represents the middle point of the surface rupture (Azzaro, 1999); F_1–F_2, coordinates of the fault tips representative of the linear source (see text). Other events with I_0 = VI considered for the isotropic model are indicated only by the identification number in the CMTE catalogue: 519, 689, 840, 949, 1450, 1451, 1454, 1459, 1476, 1497, 1583, 1595, 1635, 1641, 1713, 1749, 1754, 1759, 1765, 1773.

Date	I_0	E_0	F_1	F_2
(y/m/d)		(isotropic model)	(anisotropic model)	
1875/01/07	VII		38.638, 15.119	37.623, 15.135
1881/02/12	VII		37.710, 15.161	37.692, 15.170
1909/10/21	VII	37.655, 15.162	37.667, 15.159	37.651, 15.163
1950/04/08	VII		37.712, 15.160	37.694, 15.169
1973/08/03	VII	37.650, 15.157		
1973/08/18	VII	37.666, 15.165	37.671, 15.166	37.654, 15.171
1984/06/19	VII	37.636, 15.131		
1984/10/19	VII	37.694, 15.103		
1985/12/25	VII	37.805, 15.048		
1986/02/02	VII	37.653, 15.163		
1986/10/29	VII	37.806, 15.051		
1989/01/29	VII	37.705, 15.165		
1889/12/25	VII–VIII	37.651, 15.156	37.661, 15.142	37.639, 15.165
1898/05/14	VII–VIII	37.615, 14.889		
1907/12/07	VII–VIII	37.632, 15.134	37.646, 15.118	37.632, 15.134
1920/09/26	VII–VIII	37.713, 15.161	37.706, 15.163	37.685, 15.173
1952/03/19	VII–VIII	37.660, 15.147	37.674, 15.129	37.645, 15.160
1865/08/19	VIII	37.641, 15.165	37.653, 15.151	37.636, 15.170
1971/04/21	VIII	37.714, 15.148	37.729, 15.143	37.703, 15.150
1984/10/25	VIII	37.660, 15.095	37.665, 15.086	37.654, 15.099
2002/10/27	VIII	37.803, 15.055		
2002/10/29	VIII	37.674, 15.143	37.687, 15.133	37.659, 15.162
1879/06/17	VIII–IX	37.678, 15.143		
1894/08/08	VIII–IX	37.653, 15.110	37.660, 15.093	37.631, 15.127
1911/10/15	VIII–IX	37.699, 15.154	37.720, 15.144	37.671, 15.158
1865/07/19	IX	37.702, 15.153	37.727, 15.143	37.675, 15.158
1914/05/08	IX–X	37.659, 15.149	37.678, 15.122	37.657, 15.147

and to use the mode (intensity with the highest probability) of this distribution to forecast the intensity that could be produced at distance d from the epicentre of a given event of intensity I_0.

In our analysis we apply this procedure to the 44 earthquakes reported in Table 1 (isotropic model, column E_0, and those listed in the caption). Like I_s we consider I_0 as a discrete variable and therefore, rounding it down, we obtain three datasets of 20, 14, 8 and 2 earthquakes with I_0 VI, VII, VIII and IX, respectively. For each I_0, through Eq. (4), we estimate the parameter $\hat{p}_j, j = 1, \ldots 25$, at each of the $L = 25$ bins with width 1 km drawn around the epicentre, and then, approximate these values through the inverse power function $g(d) = (\gamma_1/d)^{\gamma_2}$. The parameters γ_1 and γ_2 for each I_0 class, obtained by the method of least squares, are reported in Table 2. By substituting the resulting value $g(d)$ in Eq. (5), we obtain the probability function of I_s at any distance d from the epicentre, conditioned on the epicentral intensity (Fig. 2).

To judge the predictive power of this method, we perform a retrospective analysis by comparing the observed macroseismic fields of the historical earthquakes with the forecast ones, on the basis of three validation criteria, two probabilistic and one deterministic (see Rotondi and Zonno, 2004). In brief, the first is the logarithmic scoring rule based on the logarithm of the likelihood function expressed through the smoothed binomial distribution:

$$score_{\text{bin}} = -\frac{1}{N}\log\prod_{n=1}^{N}\binom{I_0}{I_s^{(n)}} g(d_n)^{i_s^{(n)}}\left(1-g(d_n)\right)^{\left(I_0 - i_s^{(n)}\right)} \quad (6)$$

N being the number of felt reports and d_n the distance of the nth site from the epicentre. The second probabilistic criterion is given by the $p(A)/p(B)$ ratio between the probability that the fitted model assigns to the realisation A and the probability of the predicted value B:

$$odds_{\text{bin}} = -\frac{1}{N}\log\prod_{n=1}^{N}\frac{Pr_{\text{smooth}}\left(i_s^{(n)}\middle|D\right)}{Pr_{\text{smooth}}\left(i_{\text{smooth}}^{(n)}\middle|D\right)} \quad (7)$$

where $i_{\text{smooth}}^{(n)}$ denotes the mode of the smoothing binomial distribution (Eq. (2)) at the nth site, estimator of I_s. Finally, the deterministic criterion measures the absolute discrepancy between observed and estimated intensities at a site:

$$diff_{\text{bin}} = 1/N\sum_{n=1}^{N}\left|i_s^{(n)} - i_{\text{smooth}}^{(n)}\right|. \quad (8)$$

Table 3 shows the values of the validation criteria obtained for the earthquake with $I_0 \geq$ VII EMS. The absolute discrepancy *diff* (Eq. (8)) allows to compare the reliability of the results between our probabilistic approach and the deterministic method using the attenuation relationship

$$\Delta I = 0.98\log d + 1.01 \quad (9)$$

valid for the Etna area (Azzaro et al., 2006). The smaller the values, the better the performance of the model. As for the *odds* probabilistic criterion (Eq. (7)) we note that, being roughly $p(A) \approx \exp(-\mu_{\text{odds}})p(B)$ where μ_{odds} is the mean of the *odds* values, the fitted model assigns on average to the observed macroseismic fields about 70% of the probability of the predicted ones.

Table 2
Parameters of the inverse power function in the isotropic model.

I_0	γ_1	γ_2
VII	0.686	0.221
VIII	0.679	0.224
IX	0.727	0.254

3.2. Anisotropic model

In this paragraph, we tackle the problem of the intensity attenuation under the assumption of a linear source model; as previously explained, the preferential direction of propagation of seismic energy along strike is a condition at Etna that is more evident the stronger the earthquake. In such a case, the decay of intensity according to two different trends produces, in the simulated macroseismic field, elliptical isoseismal lines. In our model this means substituting the circular spreading from the epicentre with an ellipse whose major axis corresponds to the fault segment ruptured during the earthquake, and the source directivity (i.e. the minimum attenuation direction) is defined by the fault strike. To this end, starting from the parameters of all the surface fault ruptures reported for the historical and recent earthquakes in Azzaro (1999), we calculate the mean rupture characteristic for each epicentral intensity degree. The obtained lengths (median value) – I_0 VII = 2.5 km, I_0 VIII = 4.5 km, and I_0 IX = 6.0 km – are then used to represent the extension of the linear source in the anisotropic model. The dip of the fault plane is considered vertical.

A critical aspect concerns how to exploit the prior knowledge obtained for the volcanic areas under the isotropic assumption (Zonno et al., 2008; Rotondi et al., 2009). Hence, we apply a transformation to the plane so that the ellipse having major axis equal to the rupture length and minor axis equal to 1 km (width of the distance bin), becomes the unit circle. In this way we are able to apply the same probabilistic model defined in the isotropic case to the so-transformed data points, to estimate a new probability distribution of the site intensity, and to associate the new estimates with the original locations. An example of this transformation is illustrated

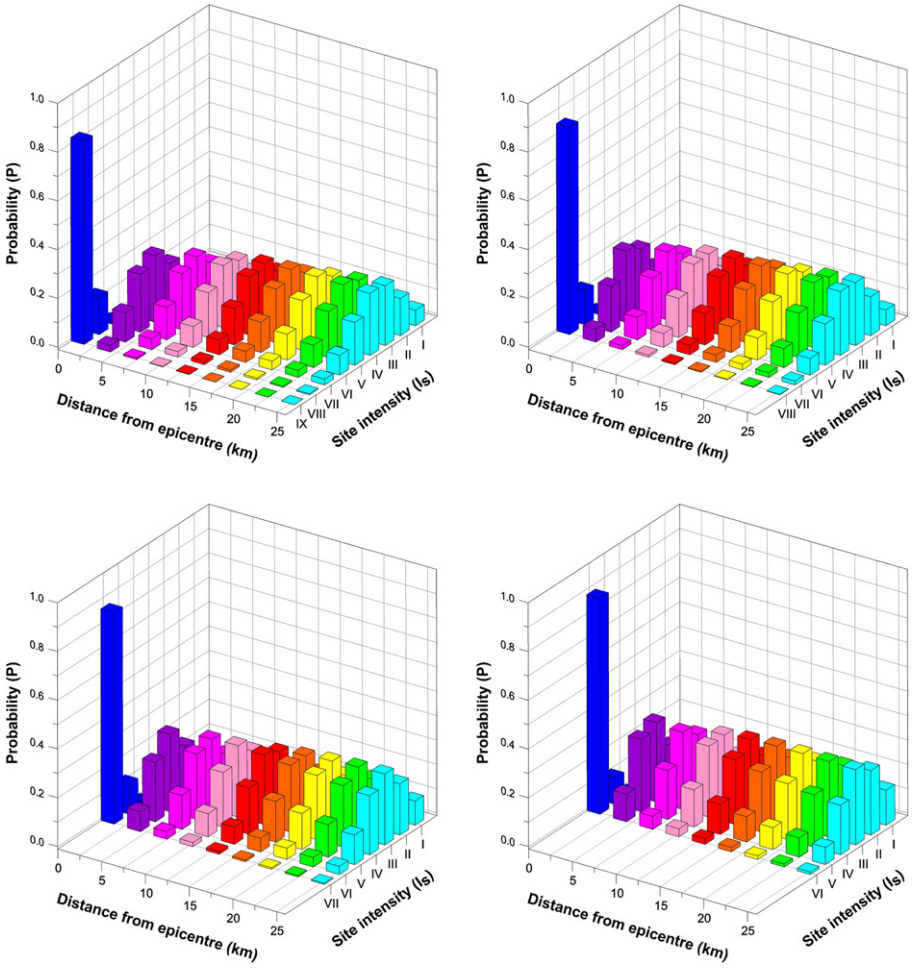

Fig. 2. Plug-in binomial probability (P) distributions of the intensity I_s at a given site as a function of its distance from the epicentre and the epicentral intensity I_0 of the earthquake.

Table 3
Values of the validation criteria for the isotropic model (point source), compared with the deterministic relationship (Azzaro et al., 2006). N_{ip} number of intensity data points in the observed macroseismic field.

Date		Binomial-beta prob. model			Logarithmic rel.
	N_{ip}	*score*	*odds*	*diff*	*diff*
1909/10/21	13	1.108	0.123	0.192	0.231
1973/08/03	33	1.286	0.225	0.439	0.439
1973/08/18	17	1.182	0.158	0.500	0.353
1984/06/19	35	1.399	0.274	0.757	0.600
1984/10/19	93	1.340	0.164	0.634	0.435
1985/12/25	10	1.221	0.041	0.250	0.600
1986/02/02	36	1.497	0.502	0.833	0.569
1986/10/29	34	1.253	0.023	0.250	0.529
1989/01/29	67	1.363	0.264	0.545	0.373
1889/12/25	24	1.216	0.132	0.604	0.792
1898/05/14	16	1.390	0.219	0.812	0.625
1907/12/07	17	1.237	0.228	0.676	0.676
1920/09/26	14	1.352	0.195	0.821	0.821
1952/03/19	98	1.423	0.282	0.934	0.786
1865/08/19	15	1.414	0.360	0.700	0.633
1971/04/21	11	1.690	0.917	0.773	0.682
1984/10/25	105	1.348	0.142	0.543	0.671
2002/10/27	17	1.325	0.052	0.382	0.353
2002/10/29	37	1.481	0.349	0.730	0.635
1879/06/17	25	1.442	0.333	0.740	0.860
1894/08/08	41	1.292	0.143	0.659	0.671
1911/10/15	41	1.471	0.295	0.854	1.073
1865/07/19	27	1.858	0.710	1.148	1.296
1914/05/08	80	1.647	0.388	0.875	0.994

in Fig. 3 and consists of the following steps: (1) rotation of the ellipse of semimajor and semiminor axes $a=2.023$ and $b=1$ km long respectively, and azimuth 2.356 rad (135°) counterclockwise by 0.785 rad (45°) so as to move the point $P_1(x_1, y_1)$ to the position $P_2(x_2, y_2)$, through the equations:

$$\begin{cases} x_2 = \cos(-\psi)x_1 - \sin(-\psi)y_1 \\ y_2 = \sin(-\psi)x_1 + \cos(-\psi)y_1 \end{cases} \quad (10)$$

being ψ the angle between the positive semi-axis x and the directrix; (2) then shrinkage of the major axis bringing $P_2(x_2, y_2)$ to $P_3(x_3, y_3)$ by $x_3 = x_2 \times b/a$ and $y_3 = y_2$; and (3) lastly, rotation of the circle clockwise so that the point P_3 goes to the point $P_4(x_4, y_4)$ by the equations:

$$\begin{cases} x_4 = \cos(\phi)x_3 - \sin(\phi)y_3 \\ y_4 = \sin(\phi)x_3 + \cos(\phi)y_3 \end{cases} \quad (11)$$

being $\phi = \arctan(y_3/x_3) - \arctan(y_2/x_2) + |\psi|$.

Since the asymmetry is more evident for the highest intensities and it decreases moving away from the epicentre, both the axes of the subsequent ellipses are increased by the same quantity – width of the bin – so that the eccentricity $e_j = \sqrt{1-(b_j/a_j)^2}$ tends towards 0 for increasing j, $j = 1,2,\ldots,L$.

This procedure is applied to the 17 earthquakes listed in Table 1 (anisotropic model, columns F_1–F_2). By using the probabilistic method described in Section 3.1, we obtain the estimates of the γ_1 and γ_2 parameters of the inverse power function (Table 4) and, substituting

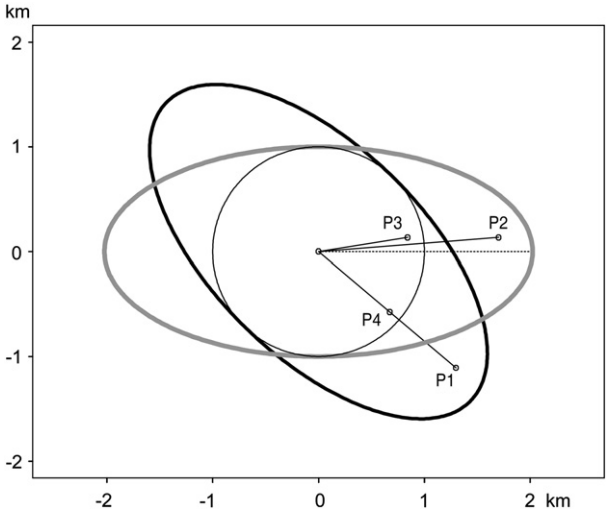

Fig. 3. Example of transformation of the ellipse (in black, semimajor axis $a = 2.023$ km, semiminor axis $b = 1$ km) into a circle with radius of 1 km. Ellipse azimuth = 2.356 rad, rotation into grey ellipse by $\psi = -0.875$ rad.

Table 5
Values of the validation criteria for the anisotropic model (linear source), compared with the deterministic relationship (Azzaro et al., 2006). N_{ip} number of intensity data points in the observed macroseismic field.

Date		Binomial-beta prob. model			Logarithmic rel.
	N_{ip}	*score*	*odds*	*diff*	*diff*
1875/01/07	7	1.148	0.191	0.571	0.500
1881/02/12	8	1.668	0.894	0.938	0.750
1909/10/21	13	1.250	0.317	0.115	0.231
1950/04/08	7	1.415	0.616	0.786	0.643
1973/08/18	18	1.255	0.266	0.556	0.361
1889/12/25	25	1.196	0.126	0.600	0.820
1907/12/07	18	1.169	0.182	0.611	0.722
1920/09/26	15	1.189	0.118	0.400	0.867
1952/03/19	99	1.412	0.286	0.922	0.766
1865/08/19	15	1.523	0.548	0.700	0.633
1971/04/21	11	2.120	1.534	0.955	0.682
1984/10/25	105	1.352	0.155	0.552	0.671
2002/10/29	38	1.468	0.425	0.605	0.618
1894/08/08	42	1.193	0.129	0.512	0.651
1911/10/15	42	1.416	0.306	0.707	1.085
1865/07/19	27	1.991	1.086	1.296	1.296
1914/05/08	81	1.486	0.285	0.756	1.019

the resulting $g(d) = (\hat{\gamma}_1/d)^{\hat{\gamma}_2}$ in Eq. (5), we estimate the probability function of I_s at any site d km far from the epicentre in the transformed plane.

The values obtained from the validation criteria for each earthquake of the considered dataset, are shown in Table 5. In the anisotropic case, the comparison between probabilistic and deterministic methods based on the *diff* criterion (Eq. (8)), indicates a better performance of the probabilistic approach. Moreover, as for the *odds* probabilistic criterion (Eq. (7)), the fitted model assigns on average to the observed macroseismic fields more than 64% of the probability of the predicted ones.

Fig. 4 highlights the improvements achieved by following the anisotropic assumption in the estimate of the macroseismic field of the 1911 Fondo Macchia earthquake, occurred in the eastern flank of Mt. Etna along the Moscarello fault with an epicentral intensity I_0 = VIII–IX EMS. In particular, the observed historic macroseismic field is compared with the synthetic intensity fields estimated according to the isotropic and anisotropic assumptions. Note that the simulation obtained by the anisotropic model fits better to the historic intensity distribution in the near-field along strike, where relevant damage (I VIII EMS) has been actually observed.

4. Application to seismic scenarios

The probabilistic method presented in this study allows, both in the case of point source (isotropic model) and linear source (anisotropic model), a complete treatment of the uncertainty. This means that not only is the intensity at any site I_s estimated, but also the entire probability distribution from which it is possible to draw measurements of dispersion or variability, such as the standard deviation or the interquartile range. The two described attenuation models are implemented in the software PROSCEN (PRObabilistic SCENario), compiled in FORTRAN for PC environment (Rotondi and Zonno, 2010), aimed at producing seismic scenarios.

Table 4
Parameters of the inverse power function in the anisotropic model.

I_0	γ_1	γ_2
VII	0.772	0.238
VIII	0.589	0.219
IX	0.728	0.259

The computation procedure is developed by two modules: as a first step, starting from the epicentral parametres of the earthquake to be simulated – the epicentral intensity I_0 (or the equivalent magnitude), the coordinates of the epicentre (point source) or the fault tips (linear source) – the software estimates the probability distribution of the macroseismic intensity on a given set of localities, for example to reproduce the macroseismic field of an historical earthquake, or on a grid map. Then, once the probability and intensity thresholds are fixed, the programme generates the expected seismic scenario which can be represented as (1) the intensity that may be reached with the fixed probability threshold and, vice versa, (2) the probability that the site intensity exceeds the fixed degree.

Fig. 5 illustrates an example of simulation carried out for an earthquake with epicentral intensity I_0 IX EMS, located in the eastern flank of Mt. Etna. We chose an event similar to the 1914 Linera earthquake, which is known as the largest shock to have occurred in the area since early 1800s (Azzaro, 2004); as for the seismic source, we confirm the S. Tecla fault, that in the short-term presents the highest time-dependent probability of rupture forecast for earthquakes with $I_0 \geq$ VIII EMS (Azzaro et al., 2012). The maps show the results calculated on a grid with node distances of 1 km according to the isotropic and anisotropic models, and different probabilities at most 25, 50 and 75%. The mode of the predictive distribution represents the intensity with the highest probability, which is assumed as the expected site intensity I_s, while the 1st and 3rd quartiles provide an estimate of the uncertainties. The ShakeMaps obtained from a point source vs a finite rupture segment (Fig. 5), show substantial differences mainly in the near-field (VII $\leq I_s \leq$ IX), where the highest values of intensity are more realistically distributed along strike, while for lower degrees the source effect progressively reduces to disappear in the far-field. Moreover, the seismic scenarios obtained with both models confirm that the severely hit area remains fairly limited also taking into account the uncertainties, since the isoseismals of highest degrees shift at least by ca. 2 km by comparing the maps of the 25–75 percentiles. Conversely, the differences are much more evident in the far-field, but this is trivial for the scenario since it involves only the felt area. However, it should be stressed that the city of Catania, located 17 km away from the epicentre, remains beyond the hazard area also considering the uncertainty related to the 25 percentile. From the point of view of seismic scenarios, this finding is consistent with the seismic history of Catania determined by the local shallow seismicity, with no damage effect reported during the last centuries (Azzaro et al., 1999; CMTE Working Group, 2008).

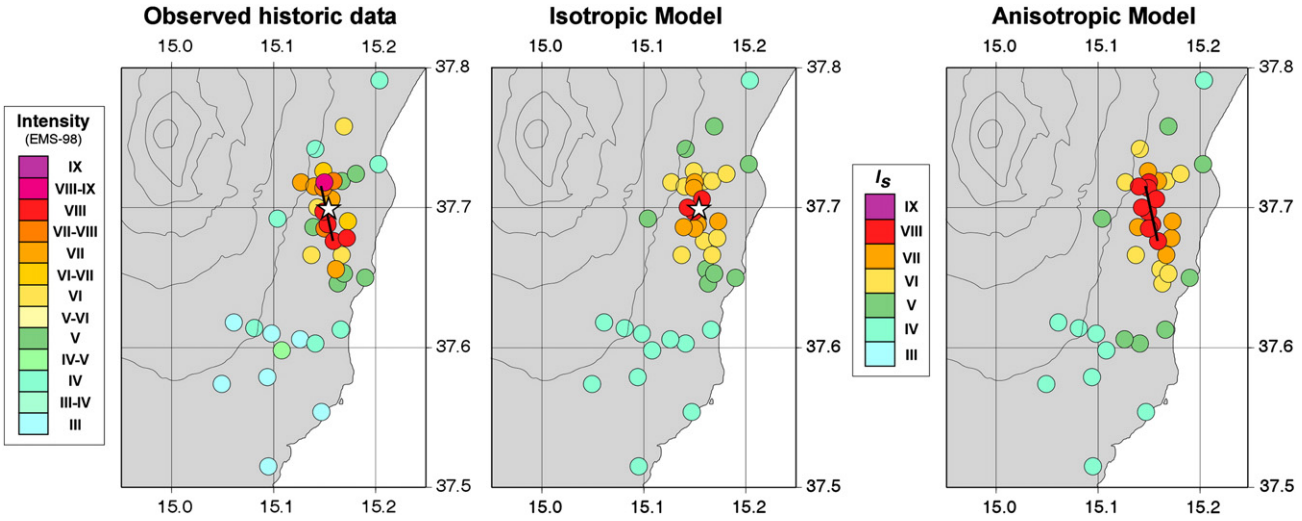

Fig. 4. October 15, 1911 Fondo Macchia earthquake (epicentral intensity I_0 = VIII–IX EMS): observed historic macroseismic field and synthetic intensity fields estimated according to the isotropic and anisotropic models. Epicentre and fault rupture are indicated by a white star and a black line, respectively; the mode of the distribution is taken as the expected intensity I_s at a site.

Fig. 6 illustrates the probability distribution of having intensities at a site I_s larger than a fixed value. The maps, referred to the same I_0 IX earthquake discussed before and calculated on a grid according to the two attenuation models, represent the three intensity classes relevant for a seismic scenario (i.e. the damage threshold $I_s \geq$ VI EMS). It is evident how the highest values of probability significantly vary in short distances, and they are fairly well confined to the near-field. This information may be useful for civil protection authorities to represent the uncertainty associated to the damage scenario for a given intensity degree on a map and adopt cautionary measures.

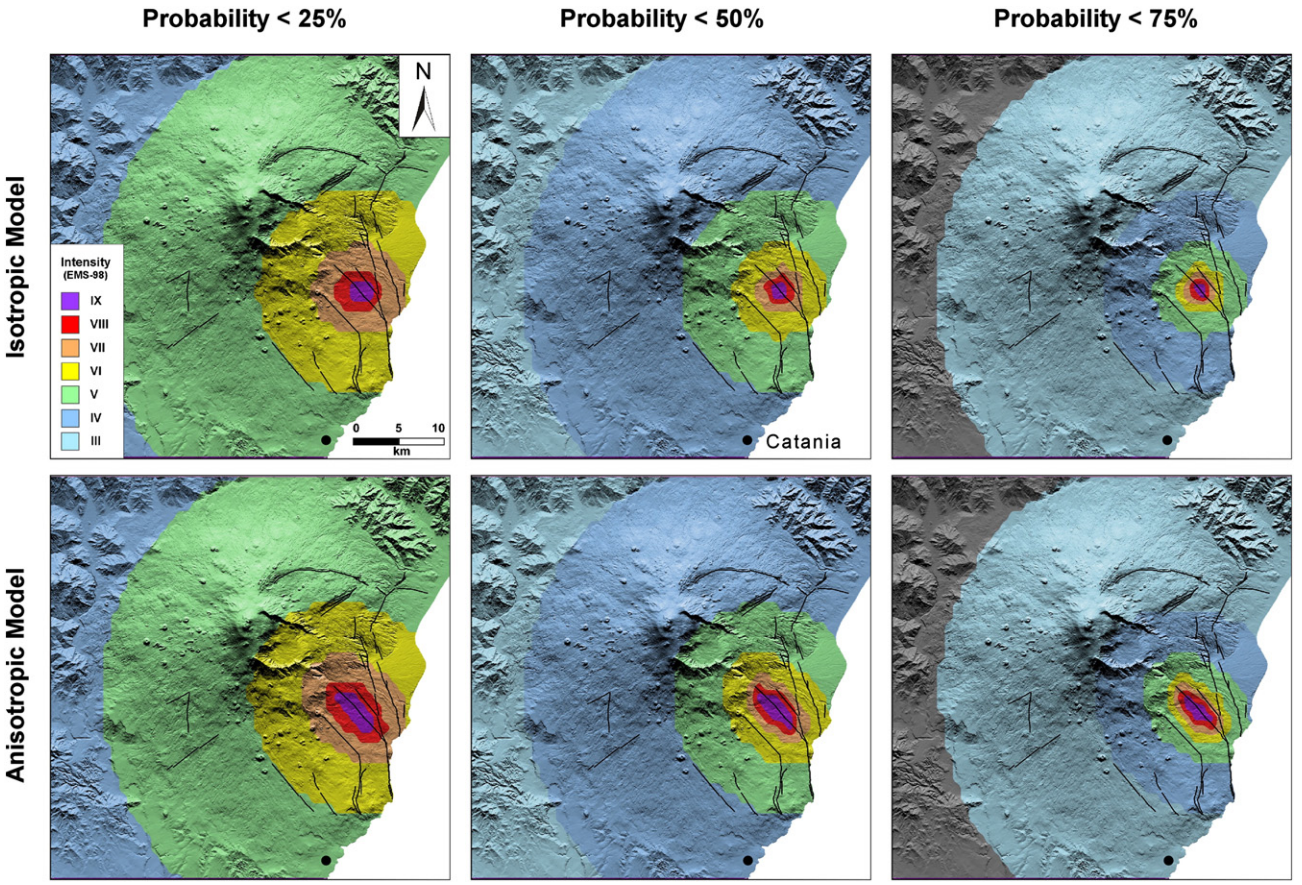

Fig. 5. Scenario for an earthquake with epicentral intensity I_0 IX EMS located in the eastern flank of Mt. Etna, along the S. Tecla fault, simulated according to a point source model (isotropic) vs a linear finite fault (anisotropic model). The maps show the site intensity exceeded with probability at most 25, 50, and 75%. The mode of the distribution is taken as the expected intensity I_s (central maps); an estimate of the uncertainties may be obtained by comparing the maps calculated for different probabilities. The grid has a node distance of 1 km.

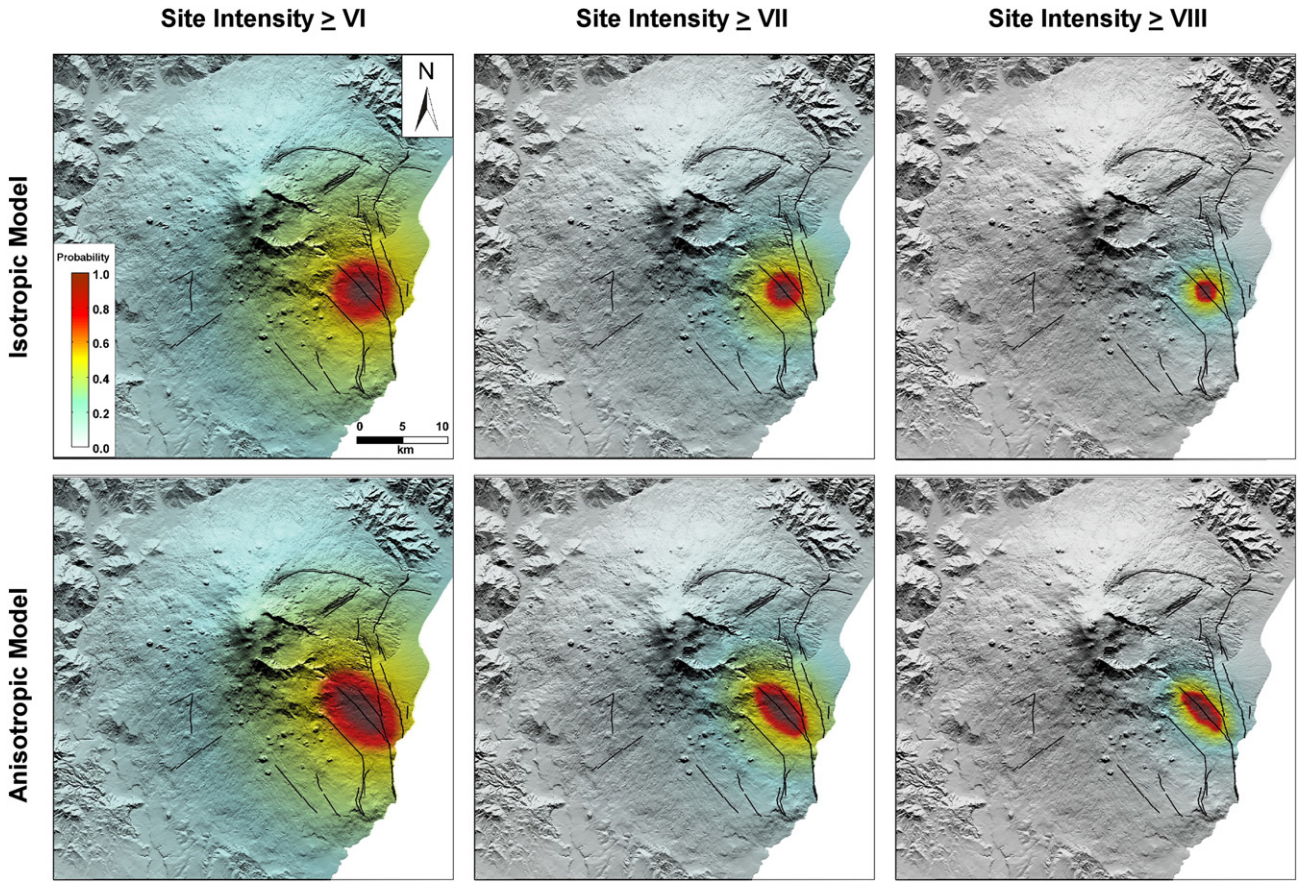

Fig. 6. Distribution of the exceeding probabilities for fixed intensity values, referred to the same earthquake in Fig. 5 (I_0 IX EMS) and both models of attenuation. The grid has a node distance of 1 km.

The comparison of the results obtained from the proposed probabilistic models with the deterministic method, is reported in Table 6. We express the average performance of the approaches through the minimum, mean, maximum, and standard deviation of the values of absolute discrepancy *diff* (Eq. (8)) calculated for the earthquakes in Tables 3 and 5. As for the isotropic model, it is evident that the mean discrepancy is rather similar but the dispersion of the values obtained by the probabilistic method, is lower. In the case of the anisotropic model, the comparison is more clearly in favour of the probabilistic approach, as indicated by the least mean discrepancy. Finally, we compare the average performance of the two probabilistic models by computing the mean discrepancy *diff* on the same earthquake dataset: 0.729 for the isotropic model, and 0.681 for the anisotropic one. This finding confirms that the simulations based on linear sources (extended finite faults) provide a more reliable estimation.

5. Conclusions

In this paper, we present a procedure that, through the probabilistic analysis of the seismic attenuation, allows estimating probabilistic seismic scenarios in the volcanic region of Mt. Etna. Using a dataset of earthquakes selected from the local catalogue, we update the binomial-beta model of intensity attenuation used at a national scale and estimate the probability distribution of the macroseismic intensity I_s at any site for different epicentral intensities I_0 and distances from the epicentre. In order to take account of the source effect, particularly evident at Etna for shallow-high intensity earthquakes, we consider two different models of attenuation: (1) isotropic, in which the source is assumed as a point and the decay comparable to a symmetric spreading (circular); (2) anisotropic, where the source is a linear finite fault and the decay depends on its direction (elliptical).

The backward validation of the results, carried out through the comparison between the macroseismic fields of historical earthquakes with the synthetic intensity maps obtained from our probabilistic approach and the deterministic law by Azzaro et al. (2006), in general shows a better performance of the probabilistic models proposed in this study. In particular, the simulations obtained by the anisotropic model are preferable when considering a specific scenario earthquake, since a more reliable distribution of the expected effects in the near-field is obtained. In this case, it is required that a causative fault must be assumed and its strike defined. Conversely, the isotropic model may be more usefully applied in situations where the seismic source is not a-priori defined.

The seismic scenarios are obtained through the software PROSCEN, a PC programme specifically compiled to calculate probabilistic intensity ShakeMaps at Etna according to the procedures and models above described. The results can be presented as (1) the intensity that may be reached with a determined probability threshold or, (2) the probability that the expected intensity exceeds a fixed degree. PROSCEN may represent an additional tool for the multi-parametric monitoring system of Etna volcano operating at INGV—Catania data acquisition centre (Andò

Table 6
Summaries of the values reported in Tables 3 and 5 for *diff* criterion for the probabilistic (binomial-beta model) and deterministic (logarithmic relationship) methods.

Model	Method	Min	Mean	Max	St. dev.	Weighted mean[a]
Isotropic	Probabilistic	0.192	0.652	1.148	0.233	0.686
(Point source)	Deterministic	0.231	0.654	1.296	0.245	0.671
Anisotropic	Probabilistic	0.115	0.681	1.296	0.260	0.703
(Linear source)	Deterministic	0.231	0.724	1.296	0.255	0.783

[a] The mean is weighted with respect to the number of intensity data points.

and Pecora, 2006; Di Grazia et al., 2009; Scollo et al., 2009; Langer et al., 2010; Montalto et al., 2010). Using as input data the instrumental parameters calculated by the automatic earthquake processing system (Patanè et al., 2002), real-time probabilistic intensity ShakeMaps can be obtained by the isotropic model for $M_L > 3.2$ earthquakes, i.e. the magnitude equivalent to I_0 VI according the new I–M relationships calibrated for this region (Azzaro et al., 2011). This value corresponds to the threshold of damage to ordinary buildings, an important scenario for civil protection purposes in order to undertake any eventual first intervention.

Not only has this probabilistic approach produced reliable simulations of seismic scenarios at a local scale, shedding more light on the role of the seismic source model in the attenuation process, but it has also provided a matrix of values of the predictive probability function of I_s. These can then be directly applied to compute the probabilistic seismic hazard at the site using the numerical procedure implemented in the software 'SASHA' (D'Amico and Albarello, 2008), thus improving the previous estimations obtained by Azzaro et al. (2008) through the deterministic attenuation relationship.

Acknowledgements

This work was funded by the Italian Dipartimento della Protezione Civile in the frame of the 2007–2009 Agreement with Istituto Nazionale di Geofisica e Vulcanologia — INGV, project V4: "Hazard connected to the flank dynamics of Etna". D. Gospodinov and two anonymous referees are thanked for their suggestions that improved the manuscript.

References

Albarello, D., D'amico, V., 2004. Attenuation relationship of macroseismic intensity in Italy for probabilistic seismic hazard assessment. Bollettino di Geofisica Teorica ed Applicata 45 (4), 271–284.

Albarello, D., D'Amico, V., 2005. Validation of intensity attenuation relationships. Bulletin of the Seismological Society of America 95, 719–724.

Andò, B., Pecora, E., 2006. An advanced video-based system for monitoring active volcanoes. Computer & Geoscience 32, 85–91.

Azzaro, R., 1999. Earthquake surface faulting at Mount Etna volcano (Sicily) and implications for active tectonics. Journal of Geodynamics 28, 193–213.

Azzaro, R., 2004. Seismicity and active tectonics in the Etna region: constraints for a seismotectonic model. In: Bonaccorso, A., Calvari, S., Coltelli, M., Del Negro, C., Falsaperla, S. (Eds.), American Geophysical Union, Geophysical monograph, 143, pp. 205–220. doi:10.1029/143GM13.

Azzaro, R., Barbano, M.S., Moroni, A., Mucciarelli, M., Stucchi, M., 1999. The seismic history of Catania. Journal of Seismology 3 (3), 235–252.

Azzaro, R., Barbano, M.S., Antichi, B., Rigano, R., 2000. Macroseismic catalogue of Mt. Etna earthquakes from 1832 to 1998. Acta Vulcanologica 12 (1), 3–36 CD-ROM.

Azzaro, R., Barbano, M.S., D'Amico, S., Tuvè, T., 2006. The attenuation of the seismic intensity in the Etna region and comparison with other Italian volcanic districts. Annales Geophysicae 49 (4/5), 1003–1020.

Azzaro, R., Barbano, M.S., D'Amico, S., Tuvè, T., Albarello, D., D'Amico, V., 2008. First studies of probabilistic seismic hazard assessment in the volcanic region of Mt. Etna (Southern Italy) by means of macroseismic intensities. Bollettino di Geofisica Teorica e Applicata 49 (1), 77–91.

Azzaro, R., D'Amico, S., Tuvè, T., 2011. Estimating the magnitude of historical earthquakes from macroseismic intensity data: new relationships for the volcanic region of Mount Etna (Italy). Seismological Research Letters 82 (4), 520–531.

Azzaro, R., D'Amico, S., Peruzza, L., Tuvè, T., 2012. Earthquakes and faults at Mt. Etna: problems and perspectives for a time-dependent probabilistic seismic hazard assessment in a volcanic region. Bollettino di Geofisica Teorica ed Applicata (1), 75–88.

CMTE Working Group, 2008. Catalogo Macrosismico dei Terremoti Etnei, 1832–2008. INGV, Catania. http://www.ct.ingv.it/ufs/macro/.

CPTI Working Group, 2004. Catalogo Parametrico dei Terremoti Italiani, version 2004 (CPTI04). INGV, Milan. http://emidius.mi.ingv.it/CPTI/.

D'Amico, V., Albarello, D., 2008. SASHA: a computer program to assess seismic hazard from intensity data. Seismological Research Letters 79 (5), 663–671.

R Development Core Team, 2008. A Language and Environment for Statistical Computing. R Foundation for Statisticsal computing, Vienna, Austria3-900051-07-0. http://www.R-prokect.org/.

Di Grazia, G., Cannata, A., Montalto, P., Patanè, D., Privitera, E., Zuccarello, L., Boschi, E., 2009. A multiparameter approach to volcano monitoring based on 4D analyses of seismo-volcanic and acoustic signals: the 2008 Mt. Etna eruption. Geophysical Research Letters 36. doi:10.1029/2009GL039567.

Faccioli, E., 2006. Seismic hazard assessment for derivation of earthquake scenarios in Risk-UE. Bulletin of Earthquake Engineering 4, 341–364.

Faccioli, E., Pessina, V., Calvi, G.M., Borzi, B., 1999. A study on damage scenarios for residential buildings in Catania city. Journal of Seismology 3, 327–343.

Faenza, L., Michelini, A., 2010. Regression analysis of MCS Intensity and ground motion parameters in Italy and its application in ShakeMap. Geophysical Journal International 180 (3), 1138–1152.

Galluzzo, D., Zonno, G., Del Pezzo, E., 2008. Stochastic finite-fault ground-motion simulation in a wave-field diffusive regime: case study of the Mt. Vesuvius volcanic area. Bulletin of the Seismological Society of America 98 (3), 1272–1288.

Giampiccolo, E., D'Amico, S., Patanè, D., Gresta, S., 2007. Attenuation and source parameters of shallow microearthquakes at Mt. Etna volcano (Italy). Bulletin of the Seismological Society of America 97 (1B), 184–197.

Grünthal, G., 1998. European Macroseismic Scale 1998 (EMS-98) European Seismological Commission, subcommission on Engineering Seismology, working Group Macroseismic Scales. Conseil de l'Europe, Cahiers du Centre Européen de Géodynamique et de Séismologie, 15, Luxembourg, p. 99. http://www.ecgs.lu/cahiers-bleus/.

Kaufman, L., Rousseeuw, P.J., 1990. Finding Groups in Data. Wiley, New York.

Langer, H., Falsaperla, S., Messina, A., Spampinato, S., Behncke, B., 2010. Detecting imminent eruptive activity at Mt Etna, Italy, in 2007–2008 through pattern classification of volcanic tremor data. Journal of Volcanology and Geothermal Research. doi:10.1016/j.jvolgeores.2010.11.019.

Magri, L., Mucciarelli, M., Albarello, D., 1994. Estimates of site seismicity rates using ill-defined macroseismic data. Pageoph 143 (4), 617–632.

McNutt, S.R., 2005. Volcanic seismology. Annual Review of Earth and Planetary Sciences 32, 461–491.

Michelini, A., Faenza, L., Lauciani, V., Malagnini, L., 2008. ShakeMap implementation in Italy. Seismological Research Letters 79 (5), 689–698.

Milana, G., Rovelli, A., De Sortis, A., Calderoni, G., Coco, G., Corrao, M., Marsan, P., 2008. The role of long-period ground motions on magnitude and damage of volcanic earthquakes on Mt. Etna, Italy. Bulletin of the Seismological Society of America 98 (6), 2724–2738.

Montalto, P., Cannata, A., Privitera, E., Gresta, S., Nunnari, G., Patanè, D., 2010. Towards an automatic monitoring system of infrasonic events at Mt. Etna: strategies for source location and modelling. Pure and Applied Geophysics 167, 1215–1231. doi:10.1007/s00024-010-0051-y.

Pasolini, C., Gasperini, P., Albarello, D., Lolli, B., D'Amico, V., 2008a. The attenuation of seismic intensity in Italy, part I: theoretical and empirical backgrounds. Bulletin of the Seismological Society of America 98 (2), 682–691.

Pasolini, C., Albarello, D., Gasperini, P., D'Amico, V., Lolli, B., 2008b. The attenuation of seismic intensity in Italy, part II: modeling and validation. Bulletin of the Seismological Society of America 98, 692–708.

Patanè, D., Ferrari, F., Giampiccolo, E., Gresta, S., 2002. A PC-based computer package for automatic detection and location of earthquakes: application to a seismic network in Eastern Sicily (Italy). In: Takanami, T., Kitagawa, G. (Eds.), Methods and Applications of Signal Processing in Seismic Network Operations. Lecture Notes in Earth Sciences, 98. Springer, Verlag, pp. 89–129.

Rotondi, R., Zonno, G., 2004. Bayesian analysis of a probability distribution for local intensity attenuation. Annals of Geophysics 47 (5), 1521–1540.

Rotondi, R., Zonno, G., 2010. Guidelines to use the software PROSCEN. Open Archives Earth-prints Repository, INGV, Reports. http://hdl.handle.net/2122/6726.

Rotondi, R., Tertulliani, A., Brambilla, C., Zonno, G., 2008. The intensity attenuation of Colfiorito and other strong earthquakes: the viewpoint of forecasters and data gatherers. Annals of Geophysics 51 (2/3), 499–508.

Rotondi, R., Brambilla, C., Zonno, G., Azzaro, R., D'Amico, S., 2009. Classification of macroseismic fields and forecasting of damage scenarios caused by earthquakes in Italian volcanic districts. Final Proc. Int. Conf. ECOBIOSYS, Classification and Forecasting Models, maggio 15, 2009, Milano, p. 4.

Rovelli, A., Bonamassa, O., Cocco, M., Di Bona, M., Mazza, S., 1988. Scaling laws and spectral parameters of the ground motion in active extensional areas in Italy. Bulletin of the Seismological Society of America 78, 530–560.

Scollo, S., Prestifilippo, M., Spata, G., D'Agostino, M., Coltelli, M., 2009. Monitoring and forecasting Etna volcanic plumes. Natural Hazards and Earth System Sciences 9, 1573–1585.

Sigbjörnsson, R., Ólafsson, S., Snæbjörnsson, J.Th., 2007. Macroseismic effects related to strong ground motion: a study of the South Iceland earthquakes in June 2000. Bulletin of Earthquake Engineering 5 (4), 591–608.

Wald, D.J., Quitoriano, V., Heaton, T.H., Kanamori, H., Scrivner, C.W., Worden, C.B., 1999. Trinet 'ShakeMaps': rapid generation of peak ground motion and intensity maps for earthquakes in southern California. Earthquake Spectra 15, 537–555.

Zonno, G., Meroni, F., Rotondi, R., Petrini, V., 1995. Bayesian estimation of the local intensity probability for seismic hazard assessment. Proc. of the Fifth International Conference on Seismic Zonation, Nice, October 17–19, 1995, pp. 1723–1729.

Zonno, G., Azzaro, R., Rotondi, R., D'Amico, S., Tuvè, T., Musacchio, G., 2008. Probabilistic procedure to estimate the macroseismic intensity attenuation in the Italian volcanic districts. Proc. of 14th World Conference on Earthquake Engineering, Beijing, October 12–17, 2008, p. 8. http://hdl.handle/net/2122/4212.

Zonno, G., Rotondi, R., Brambilla, C., 2009. Mining macroseismic fields to estimate the probability distribution of the intensity at site. Bulletin of the Seismological Society of America 98 (5), 2876–2892.

Zonno, G., Oliveira, C.S., Ferreira, M.A., Musacchio, G., Meroni, F., Mota-de-Sà, F., Neves, F., 2010. Assessing seismic damage through stochastic simulation of ground shaking: the case of the 1998 Faial earthquake (Azores Islands). Surveys in Geophysics 31, 361–381. doi:10.1007/s10712-009-9091-1.